D19

Experimental Investigation of the Influence of Paddy Ridges on Suspended Load Deposition During Inundation

○ Can DING, Kenji KAWAIKE, Hajime NAKAGAWA, Kazuki YAMANOI, Rocky TALCHABHADEL

Paddy field is important to people's daily life but vulnerable to flood and sedimentation. In this research, physical experiments were conducted for better understanding of the impact of paddy ridges on sediment deposition during inundation disaster. The results show that the flow near the ridges presents obvious three dimensional characteristics. Along the main flow direction, deposition happened at the ridge back, and erosion was found at the front and downstream of the ridge. Two-dimensional (2D) numerical simulation results could generally reflect the deposition area and thickness but is not sufficient for the detailed results around the ridges.

Introduction

In practical situation, paddy field is often divided by different parts by paddy ridges or roads, they play a role just like small embankment. During the flood inundation, it may not only influence the flood propagation, but also the sedimentation results. The purpose of the work is to better understand the influence of paddy ridges on sedimentation so that we can accurately predict the sediment deposition results and appropriately manage the farmland.

Experimental setup

The experimental setup was installed in Ujigawa Open Laboratory, Kyoto University. The setup consists of a 0.3m wide river and a 3m long and 1.6m wide inundated floodplain, the height of the embankment and the ridge are 15cm and 5mm, respectively, and the length of the inflow breach is 0.2m. **Fig.1** refers to the plan view of the experimental setup and the distribution of measuring points. 3 experimental cases were performed, case 1without ridges and with a 4.5cm height downstream boundary, case 2 with ridges and the same downstream boundary with case 1, case 3 with ridges and the downstream was set as open boundary. A discharge of 2L/s was given as the inflow boundary, and some relevant parameters of cases 1 and 2 are shown in **Tab.1**. In case 1 and 2, velocity and final deposition thickness were measured, but in case 3, as the water level is too small, only deposition thickness data was collected.

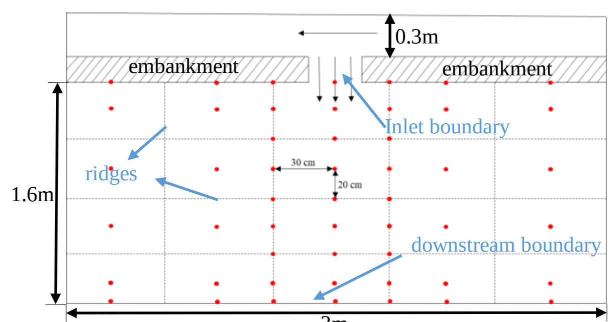

Fig.1 Plan view and the distribution of measuring points of the experimental setup

Table1. Hydraulic condition near the inlet boundary

Inflow Discharge	Mean velocity	Flow depth	Shear velocity	Critical shear velocity	Shear velocity ratio	*Fr*	Rouse Number	n	Setting velocity	Sediment density
2 L/s	19.20 cm/s	5.20 cm	1.23 cm/s	1.31 cm/s	0.93	0.27	1.53	0.02	0.75 cm/s	2.65 g/cm^3

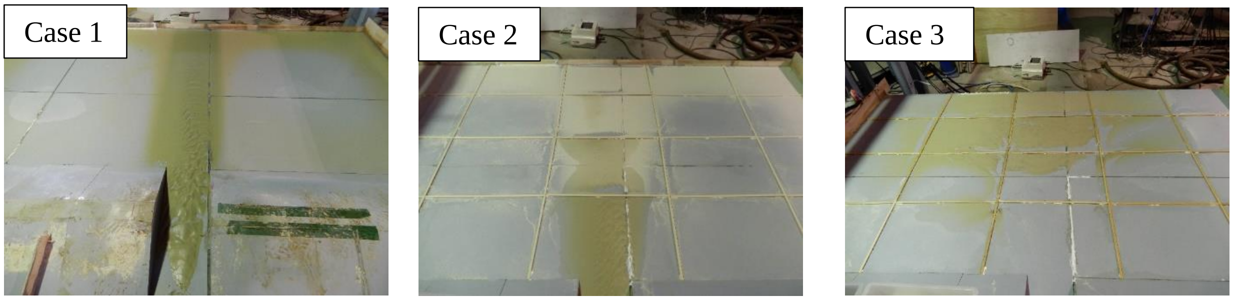

Fig.2 Final deposition results of 3 experimental cases

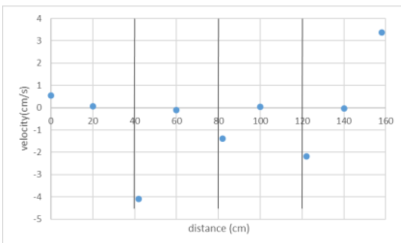

Fig.3 vertical direction velocity of each measuring point along the centerline of the setup

Results

Fig.2 shows the final deposition results of 3 experimental cases. Compare case 1 and 2, the deposition area is almost similar, most of deposition happened in the vicinity of inlet and along the main flow direction, but in case 2, it is found that deposition happened on the back side of the ridge, and erosion happened on the front side and the downstream of the ridge. **Fig.3** illustrates the process for this phenomenon. **Fig.4** shows the vertical velocity of each point along the platform centerline. For case 3, because of the open downstream boundary, high bed shear stress caused strong erosion near the inlet boundary and most of sediment was transported to downstream. Besides, through experimental observation, the flow pattern presented stronger lateral velocity in case 3, which caused obvious erosion near the side ridges. (**Fig.2 c**) A 2D numerical model was developed to simulate the corresponding experimental cases. The governing equation was expressed as:

$$\frac{\partial h}{\partial t}+\frac{\partial (hu)}{\partial x}+\frac{\partial (hv)}{\partial y}=0$$

$$\frac{\partial (hu)}{\partial t}+\frac{\partial (hu^2)}{\partial x}+\frac{\partial (huv)}{\partial y}=-gh\frac{\partial H}{\partial x}-\frac{gn^2u\sqrt{u^2+v^2}}{h^{\frac{1}{3}}}$$

$$\frac{\partial (hv)}{\partial t}+\frac{\partial (huv)}{\partial x}+\frac{\partial (hv^2)}{\partial y}=-gh\frac{\partial H}{\partial y}-\frac{gn^2\sqrt{u^2+v^2}}{h^{\frac{1}{3}}}$$

$$\frac{\partial (hc)}{\partial t}+\frac{\partial (hcu)}{\partial x}+\frac{\partial (hcv)}{\partial y}=w(c_e-c)+D(\frac{\partial^2 c}{\partial x^2}+\frac{\partial^2 c}{\partial y^2})$$

$$\frac{\partial z_b}{\partial t}+\frac{1}{1-\lambda}(\frac{\partial q_x}{\partial x}+\frac{\partial q_y}{\partial y}+w(c_e-c))=0$$

Fig.5 shows the numerical results of cases 2 and 3. The numerical results could generally reflect the deposition area and thickness, but due to the three dimensional flow characteristics near the ridges, 2D numerical model is not sufficient for the detailed results and three dimensional (3D) numerical model could be recommended.

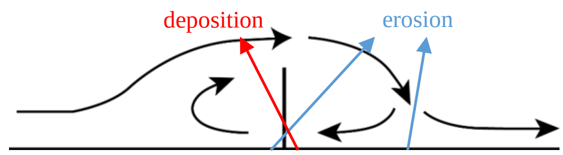

Fig.4 schematization of flow pattern around the ridges

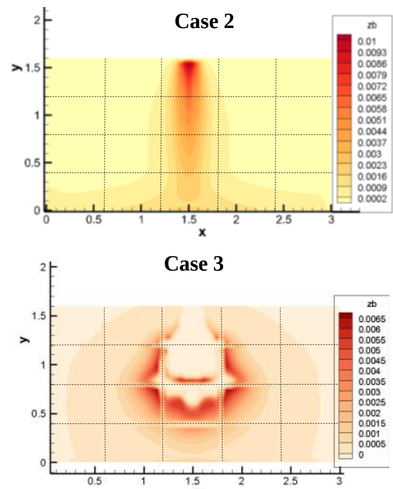

Fig.5 Numerical deposition results of cases 2 and 3

Conclusion

Physical experiments were conducted to investigate the influence of paddy ridges on suspended load deposition in this research. The results reveal that deposition and erosion happened near the ridges due to the three dimensional flow characteristics. Compared with 2D model, 3D model would be more sufficient to reproduce this phenomenon.